HHS Public Access

Author manuscript

Circ Res. Author manuscript; available in PMC 2017 September 16.

Published in final edited form as:

Circ Res. 2016 September 16; 119(7): 810–826. doi:10.1161/CIRCRESAHA.116.309094.

Rasip1-Mediated Rho GTPase Signaling Regulates Blood Vessel Tubulogenesis via Non-Muscle Myosin II

David M. Barry[1], **Yeon Koo**[1], **Pieter R. Norden**[2], **Lyndsay A. Wylie**[3], **Ke Xu**[1], **Chonlarat Wichaidit**[4], **D. Berfin Azizoglu**[1], **Yi Zheng**[5], **Melanie H. Cobb**[4], **George E. Davis**[2], and **Ondine Cleaver**[1]

[1]Department of Molecular Biology and Center for Regenerative Science and Medicine, University of Texas Southwestern Medical Center, 5323 Harry Hines Blvd., Dallas, Texas, USA 75390

[2]Department of Medical Pharmacology and Physiology, MA 415 Medical Sciences Building, University of Missouri, Columbia, MO, USA 65212

[3]Department of Biology, University of North Carolina, Chapel Hill, NC, USA

[4]Department of Pharmacology, University of Texas Southwestern Medical Center, 5323 Harry Hines Blvd., Dallas, Texas, USA 75390

[5]Div. of Experimental Hematology and Cancer Biology, Children's Hospital Research Foundation, Univ. of Cincinnati, Cincinnati, OH 45229

Abstract

Rationale—Vascular tubulogenesis is essential to cardiovascular development. Within initial vascular cords of endothelial cells (ECs), apical membranes are established and become cleared of cell-cell junctions, thereby allowing continuous central lumens to open. Rasip1 is required for apical junction clearance, as well as for regulation of Rho GTPase activity. However, it remains unknown how activities of different Rho GTPases are coordinated by Rasip1 to direct tubulogenesis.

Objective—The aim of this study is to determine the mechanisms downstream of Rasip1 that drive vascular tubulogenesis.

Methods and Results—Using conditional mouse mutant models and pharmacological approaches, we dissect GTPase pathways downstream of Rasip1. We show that clearance of EC apical junctions during vascular tubulogenesis depends on Ras interacting protein 1 (Rasip1), as well as the GTPase Cdc42 and the kinase Pak4. Genetic deletion of Rasip1 or Cdc42, or inhibition

Address correspondence to: Dr. Ondine Cleaver, Department of Molecular Biology, University of Texas Southwestern Medical Center, 5323 Harry Hines Blvd., NA8.300, Dallas, Texas 75390-9148, USA. Tel: (214) 648-1647, Fax: (214) 648-1196, ondine.cleaver@utsouthwestern.edu.

DISCLOSURES

The authors declare no competing or financial interests.

AUTHOR CONTRIBUTIONS

Most experiments were performed by D.M.B., Y.K., P.N. and L.A.W. K.X., C.W., and D.B.A. carried out supportive experiments. Y.Z. and M.H.C. provided reagents and expertise, and G.E.D. contributed to underlying ideas and analysis, and contributed 3D in vitro data. All authors read the manuscript critically. O.C. supervised the overall project and contributed to the analysis. D.M.B and O.C. wrote the manuscript.

of Pak4, all block EC tubulogenesis. By contrast, inactivation of RhoA signaling leads to vessel overexpansion, implicating actomyosin contractility in control of lumen diameter. Interestingly, blocking activity of NMII either prior to, or after, lumen morphogenesis results in dramatically different tubulogenesis phenotypes, suggesting time-dependent roles.

Conclusions—Rasip1 controls different pools of GTPases, which in turn regulate different pools of NMII to coordinate junction clearance (remodeling) and actomyosin contractility during vascular tubulogenesis. Rasip1 promotes activity of Cdc42 to activate Pak4, which in turn activates NMII, clearing apical junctions. Once lumens open, Rasip1 suppresses actomyosin contractility via inhibition of RhoA by Arhgap29, allowing controlled expansion of vessel lumens during embryonic growth. These findings elucidate the stepwise processes regulated by Rasip1 through downstream Rho GTPases and NMII.

Keywords

Rasip1; NMII; endothelial cell; tubulogenesis; actin cytoskeleton; cell signaling; vasculogenesis

INTRODUCTION

Blood vessels consist of endothelial cells (ECs), connected at their lateral edges by tight and adherens junctions (TJs and AJs). When endothelial progenitors, or angioblasts, coalesce into primitive cords, they change shape and reorganize their junctions to open, blood-carrying lumens. The formation of vascular lumens is referred to as ‘tubulogenesis’, and is essential to the passage of blood and serum. Since this process is essential to the viability of all tissues within vertebrate organisms, understanding how blood vessels develop lumens is critical to the study of embryonic development and disease.

A molecular theme underlying both epithelial and endothelial tubulogenesis is signaling by the Rho family of small GTPases[1, 2]. The most highly characterized members of this family include RhoA, Cdc42, and Rac1[3]. Previous studies using cultured ECs have shown that Cdc42 and Rac1 signaling are necessary to stimulate vascular lumen formation, whereas RhoA mediates vessel collapse and regression[4]. During EC tubulogenesis, Rho GTPase activity is regulated by several proteins, including Ras interacting protein 1 (Rasip1)[5]. Rasip1 interacts with an array of GTPases including Ras and Rap1, promoting activity of Cdc42 and Rac1, while inhibiting RhoA activity[5–9]. Rasip1 and its binding partner, the GTPase-activating protein Arhgap29, inhibit RhoA, which in turn blocks Rho associated kinase (ROCK) signaling[5, 9]. RhoA and ROCK normally activate non-muscle myosin II (NMII) via phosphorylation of its regulatory light chain (phospho myosin light chain, pMLC). NMII, in turn, controls F-actin crosslinking and contractility to regulate cell shape, adhesion and migration[10]. Previously, Rasip1 was shown to control F-actin contractility, EC-ECM adhesion maturation, and EC-EC adhesion polarity to mediate EC tubulogenesis through modulation of GTPase signaling[5, 11, 12]. However, how GTPase signaling is coordinated to influence these distinct cellular events remains unknown.

In this study, we uncover that blood vessel tubulogenesis requires two Rasip1-governed, spatio-temporally distinct GTPase signaling events that converge onto one molecular effector, NMIIA. We show that initial lumen formation depends on angioblast polarization

and cell-cell adhesion remodeling. The clearance of cell-cell adhesions from EC pre-apical membranes requires NMII-dependent actomyosin activity. This activity, in turn, is controlled by Cdc42/Rac1 via regulation of Pak4, signaling proteins downstream of Rasip1. Inhibition of this pathway results in ectopic apical junctions and blocks tubulogenesis. Once lumens open and the heart starts to beat, nascent vessels experience hemodynamic pressure due to blood flow. We show that restraint of lumen expansion occurs through membrane tension provided by NMII-mediated contractility. This NMII activity is held in check through RhoA suppression by Rasip1-Arhgap29, allowing vessels to expand over developmental time. Inhibition of Rasip1 or Arhgap29 results in narrow lumens, while inhibition of RhoA, ROCK or NMII leads to lumen dilation. We demonstrate that the balance and different timing of NMII activation through Cdc42/Pak versus RhoA/ROCK is critical for blood vessel lumen opening and expansion. This study reveals a reiterative process where GTPases control lumen morphogenesis via differential regulation of NMII activation.

METHODS

Mouse and embryo handling

All animal husbandry was performed in accordance with protocols approved by the UT Southwestern Medical Center IACUC. Embryos were dissected and fixed in 4% PFA/PBS for 40 min at 4°C, then dehydrated to 75% ethanol for storage at −20°C.

Inducible deletion of Rho GTPases in mice

To induce deletion of Cdc42, Rac1, or RhoA using CAG-CreERT2, mothers were gavaged with tamoxifen (3 mg tamoxifen/40 g mouse) at noon during stages E6.5 and E7.5, 36 hours and 12 hours before dissection respectively. Embryos were dissected at midnight at stage E8.0 ($n \geq 3$ for each line).

Whole-mount immunofluorescence in embryos

Whole-mount staining was performed as previously described[33].

Whole-mount immunocytochemistry

PECAM and PECAM/Endomucin costain (PE) was performed as previously described[33].

Immunofluorescence staining of embryonic tissues

Whole-mount staining was performed as previously described[23]. TSA immunofluorescent staining (PerkinElmer; individual fluorescein tyramide reagent pack, cat# SAT701) was used to stain pMLC.

Immunofluorescence staining of cultured ECs

Immunofluorescence staining of MS1cells was performed as previously described[23]. Staining of HUVEC in 3D collagen matrices was performed as previously described[34].

Hematoxylin and Eosin (H&E) staining

H&E staining was performed as previously described[33].

LacZ staining

Embryos were fixed using gluteraldehyde for 15 min, rinsed in PBS and stained for β-galactosidase (β-gal) overnight (overnight) as previously described[35]. Images were taken with a NeoLumar stereomicroscope (Zeiss) using a DP-70 camera (Olympus).

In situ hybridization

In situ hybridization staining on sections and whole mount were performed as previously described[36]. An Arhgap29 3' coding region fragment (1.2kb) and a Plexin D1 clone (MMM1013-66046 Open Biosystems) were used to generate Dig-labeled RNA probes.

siRNA transfection and recombinant protein expression

siGENOME siRNAs obtained from GE Dharmacon were transfected into cultured MS1 or HUVEC using standard protocols for transfection and western analysis blot, as previously described (antibodies used for western blots are detailed in supplemental material Table S1 and siRNA sequences are detailed in supplemental material Table S2)[37]. Transfection of plasmids expressing Rasip1-GFP and GFP was performed 24 hours after siRNA transfection. 1μg of plasmid DNA was transfected onto cells cultured on a 12mm cover slip using 1μg Lipofectin (Invitrogen) dissolved in 300μl Optimem. Cells were fixed and stained 24 hours after transfection.

TEM

TEM was carried out by UTSW Electron Microscopy Core Facility as per their standard protocols.

In vitro lumen formation assay

HUVEC lumen and tube formation in 3D collagen matrices were performed as previously described[37].

Whole embryo culture

WEC protocol was adapted from Mary Dickinson and James Lauderdale. Embryos expressing Flk1-eGFP were dissected with their yolk sac intact at E8.0 in DMEM containing 8% FBS and 1% antibiotic antimycotic with HEPES. The embryos were cultured for 3 hours in media containing 50% male rat serum and 50% DMEM with HEPES and antibiotics in a Precision Incubator Unit (B.T.C. Engineering Milton Cambridge England). ROCK inhibitor (Y-27632), Pak4 inhibitor (PF-03758309), Rac1-3 inhibitor (EHT), and the NMII inhibitor (blebbistatin) were all added before culture at 10μM. After culture, embryos were imaged using a Zeiss AxioObserver epifluorescence microscope then fixed at 4°C with 4% PFA/PBS for 40min.

Live imaging

Embryos expressing Flk1-eGFP were dissected with their yolk sac intact at E8.25 in DMEM containing 8% FBS and 1% antibiotic antimycotic with HEPES. The embryos were plated on glass bottom dishes coated with matrigel in media containing 50% male rat serum and

50% DMEM with HEPES. The embryos were then imaged for 4 hours using a spinning disk confocal.

Cell spreading assay

10,000 MS1 cells were seeded into a 96 well plate coated with 50μl of matrigel per well. After 24 hours of culture the cells were imaged in bright field. The area that the cells cover was quantified using ImageJ software.

Statistics

All datasets were taken from n≥3 biological replicates, with n≥5–10 fields of view analyzed. Data are presented as mean±s.e.m. All statistical analysis was performed using two-tailed, unpaired Student's t-test in Graphpad Prism software. P-values lower than 0.05 were considered statistically significant. See supplemental experimental methods for detailed statistical analysis using CellProfiler software.

RESULTS

Blood vessel lumens arise between ECs following clearance of apical adhesions

To assess morphogenesis of blood vessels, we examined vasculogenesis in Flk1-eGFP mouse embryos. Vasculogenesis first occurs in the aorta and the yolk sac at E8.0 (0–1 somite stage). As previously reported, angioblasts arise as scattered mesodermal progenitors that then assemble to form vascular cords (Figure 1A–A', B–B')[13]. Angioblasts differentiate into ECs as they flatten and form a lumen at the cord center (Figure 1A'–A'',B'–B''). This process in the aortae occurs in a progressive, anterior-to-posterior manner along the embryonic axis (Online Figure I A). By contrast, live imaging of yolk sac vessels reveals that tubulogenesis in this vascular bed occurs all at once, after the cord network has formed (Figure 1C–C' and Online video I).

To examine cellular events during lumen formation (or lumenogenesis), we analyzed EC junctions in E8.0 cords. Sections were stained for the TJ adhesion molecule zona occludens 1 (ZO-1) and the apical membrane sialomucin podocalyxin (PODXL). As angioblasts come into contact, they form adhesions between contacting membranes (Online Figure I B–D). At this 'pre-apical' surface, PODXL becomes polarized and overlaps with adhesion complex foci marked by ZO-1 (Figure 1D–D''). Transmission electron microscopy (TEM) reveals that adhesion complexes stitch ECs together at loci scattered along the pre-apical membrane, flanking 'slit-like' small luminal spaces (Figure 1G–G'). EC membrane at slits take on a concave appearance (Figure 1G'), consistent with PODXL separating apposing membranes via electrostatic repulsion[14]. Soon after initial angioblast adhesion, junctions remodel, disappearing from the cord center while enriching peripherally (Figure 1E–E'', H, Online Figure I E–E'''). During this process, ECs flatten and appear 'almond-shaped' in cross section, opening a single central lumen (Figure 1F–F'', I). En face confocal imaging of adhesions at the cord center reveal TJs clustered in ribbons that run longitudinally along pre-apical membranes (cross section view Figure 1J–L; en face view Figure 1J'–L'; Online Figure I G). As lumens open, adhesion ribbons shrink and become restricted to basolateral/

peripheral regions of the cord, clearing the apical membrane (Figure 1J'–L'). Overall, apical junctional clearance allows a central lumen to open (Figure 1M).

Failed lumens in Rasip1 nulls exhibit ectopic apical junctions

We previously showed that Rasip1 is essential for vascular tubulogenesis, and that VE-cadherin (VEcad) and ZO-1 rich adhesions are observed at the apical membrane of Rasip1$^{-/-}$ cord ECs[5, 15]. In the absence of Rasip1, blood vessels fail to open continuous lumens (Figure 2A–A'), as mutant ECs are aberrantly stitched together by ectopic apical adhesions, as shown with a PECAM/Endomucin costain (PE, both red), which are strikingly rich in F-actin (phalloidin, green) (Figure 2B–C'). Live imaging of Rasip1$^{-/-}$ yolk sac vessels similarly showed failed lumen formation, as ECs within vascular cords failed to form central lumens (Figure 2D–D' and Online video II).

To further elucidate mechanisms by which Rasip1 regulates EC lumen formation, we assessed its localization in vivo and in vitro. In aortic ECs, Rasip1 was enriched at cell-cell adhesions, as well as transiently along the apical membrane during initial lumen opening (Figure 2E–F''). Similarly, HUVEC transfected with Rasip1-GFP and plated either in monolayer cultures or in 3D collagen matrices show strong transient localization to cell-cell adhesions and to the apical membrane during lumen opening, respectively (Online Figure I F, H–I''). Both in vivo and in vitro Rasip1 was also found to localize to small round cytoplasmic structures near the apical membrane (Figure 2G–G'', Online Figure I H–I''). Previous work suggested that Rasip1 localizes to endomembranes[7]. We therefore assessed whether Rasip1 was found on cytoplasmic components such as endosomes. Rasip1 immunostaining was observed to overlap with Rab5 and Rab8, but not Rab7, suggesting it may be recruited to recycling endosomes (Online Figure I J–L). To confirm this, we expressed a constitutively active form of Rab5 (Q79L) that causes early endosomes to fuse and enlarge, and assessed Rasip1 localization. Rasip1 protein was strongly enriched in these structures (Online Figure I M–M''). Together, these results suggest that Rasip1 is recruited to endosomes as well as EC adhesions, and is later recruited to apical membrane.

Clearance of apical junctions requires actomyosin contractility

To mechanistically address how Rasip1 might remodel cord EC adhesions away from the apical membrane and restrict them to lateral boundaries, we investigated whether adhesions are normally dismantled and endocytosed, or re-localized. First, whole E8.0 cord stage embryos were cultured (WEC) for 3 hours and treated with Pitstop 2, a drug that inhibits both clathrin-mediated and clathrin-independent endocytosis[16, 17]. We found that adhesions were cleared from the apical membrane in both control and Pitstop 2-treated embryos (Online Figure II A–E). Since blocking endocytosis did not perturb adhesion removal from the apical membrane, we hypothesized that adhesions may instead move away from the apical membrane using an actomyosin-dependent force. Consistent with this idea, F-actin and active, serine phosphorylated myosin light chain (pMLC) were enriched in adhesion complexes, as the adhesions progressively cleared from cord centers (Online Figure II F–I').

To determine whether F-actin and myosin are necessary to clear apical adhesions, cord-stage embryos were treated with pharmacological inhibitors. E8.0 Flk1-eGFP WEC was

performed for 3 hours in the presence of either Cytochalasin D, which inhibits actin polymerization, or blebbistatin, which blocks NMII ATPase activity. Embryos treated with either inhibitor dramatically failed to clear apical adhesion complexes (Figure 2H–H', L–L'). Consequently, cord ECs stayed stitched together, and did not form patent lumens (Figure 2I–J', M–N'). Live imaging of Flk1-eGFP yolk sacs treated with either drug revealed that continuous vessel lumen formation never took place (Figure 2K–K', O–O' and Online video III and IV). These results suggest that F-actin and NMII-mediated F-actin contractility are both essential for remodeling of apical adhesions away from cord centers, and are thereby essential for formation of continuous lumens.

Cdc42, but not RhoA, signaling downstream of Rasip1 is required for lumen formation

We previously showed that Rasip1 regulates the activity of downstream GTPases, Cdc42, Rac1 and RhoA[5]. Indeed, Rasip1 significantly promoted activity of Cdc42 and Rac1 and the downstream kinase Pak4, while it suppressed activity of RhoA and its downstream kinase ROCK[5]. Both Cdc42-Pak and RhoA-ROCK signaling are known to play critical roles in organization of the cytoskeleton[18]. We therefore asked whether EC lumen formation required either of these two signaling cascades, by genetically ablating Cdc42, Rac1, or RhoA in mice, in endothelium prior to lumen formation. Floxed RhoA, Rac1, or Cdc42 mice (genes flanked by LoxP sequences)[19–22] were crossed to Tie2-Cre, which expresses Cre in ECs. In these embryos, although Cre is expressed in angioblasts (Online Figure III A–B), protein levels were only depleted prior to lumen formation in yolk sac vessels, but not dorsal aortic ECs (Online Figure III E–L'). To delete in aortic ECs prior to lumen formation, the inducible and ubiquitous driver CAG-CreERT2 was used. This allowed early deletion of each gene (after gastrulation, Online Figure III C–D) and efficient deletion of each protein in aortic cords prior to lumen formation, with negligible effects on non-endothelial tissues (Online Figure III, Induction diagram).

Deletion of Cdc42 in yolk sac vessels using Tie2-Cre, or in aortae using CAG-CreERT2 ($Cdc42^{CAGKO}$), led to a dramatic block in vascular lumen formation, as we previously showed (Figure 3A–C', Online Figure IV A–B')[23]. Deletion of Cdc42 blocked lumens in the anterior aortae, as well as inhibited angioblast migration in yolk sac vessels (Figure 3A–A', Online Figure IV A–A'). In posterior aortic cords, where mesoderm is still differentiating into angioblasts, loss of Cdc42 impaired migration (Online Figure IV C–D'). Similar to $Rasip1^{-/-}$ embryos, ectopic EC apical cell-cell junctions were observed in $Cdc42^{CAGKO}$ cords (Figure 3B–C', Online Figure IV E–H'). Live imaging of yolk sac vessels showed that Cdc42 deleted ECs largely fail to form vascular cords, and ECs that do form cords fail to develop lumens (Figure 3D–D' and Online video V). Cdc42-depleted yolk sac ECs displayed a slight decrease in proliferation (7.2% less) and no change in apoptosis (Online Figure IV I–T).

To assess whether the Cdc42-activated kinase Pak4 is necessary for lumen formation downstream of Rasip1 and Cdc42, WEC was performed in the presence of an inhibitor that preferentially blocks Pak4 activity (PF-03758309) for 3 hours. Treatment with the inhibitor blocked lumen formation and apical adhesion remodeling, phenocopying Rasip1 null dorsal aortae (Figure 3E–G'). Live imaging of embryos treated with the Pak4 inhibitor showed that

vascular cords failed to open any lumens (Figure 3H–H' and Online video VI). These results suggest that loss of the Cdc42-Pak4 signaling pathway activity contributes to the failed lumen formation phenotype observed in Rasip1$^{-/-}$ embryos.

In striking contrast, deletion of RhoA or Rac1 using Tie2-Cre or CAG-CreERT2 had no effect on vessel lumen formation (Figure 3I–K', Online Figure V). Although initial lumens formed normally, deletion of RhoA or Rac1 caused embryonic lethality. RhoA mutants displayed overall hypoplasia at E9.25 and Rac1 mutants at E11 (Online Figure V A–A', Online Figure VI A–A'). Deletion of RhoA or Rac1 also led to marked yolk sac vascular remodeling defects at E9.5 (Online Figure V B–B', Online Figure VI B–B'). These findings suggest that Cdc42, Rac1 and RhoA are all necessary for embryonic survival and vascular development. However, while Cdc42 specifically drives clearance of apical EC junctions, RhoA and Rac1 are not required for this process.

RhoA-ROCK-NMII signaling suppresses vessel expansion

Although RhoA was not necessary for lumenogenesis and apical junction clearance, there was a notable difference in vessel diameter of embryos lacking RhoA. RhoA-depleted aortae were on average 8.6 times larger, while RhoA-depleted yolk sac vessels were 7.2 times larger than controls (Figure 3I–K', Online Figure VI C–D). Live imaging of yolk sac vessels showed that RhoA-depleted ECs develop dramatically larger lumens (Figure 3L–L and Online video VII). At the onset of lumen formation, ECs were markedly more flattened and spread out. The average distance between EC nuclei was increased by 56%, revealing that ECs occupied a larger circumferential area (Online Figure VI E). We note that RhoA-deleted vessels also exhibited a 20% increase in pHH3 positive cells with only a slight increase in apoptosis (Online Figure VI G–N). This suggests that RhoA normally restricts lumen diameter through cell shape regulation.

Similarly, we assessed whether the RhoA effector ROCK was necessary for lumen formation. WEC was performed in the presence of the ROCK inhibitor Y-27632 for 3 hours. Inhibition of ROCK dramatically enhanced lumen formation and increased the average distance between aorta nuclei by 23%, phenocopying RhoA-deleted aortae (Figure 3M–O', Online Figure VI F). Live imaging of the yolk sac vasculature under the same conditions also showed that ROCK-inhibited ECs rapidly develop much larger lumens (Figure 3P–P' and Online video VIII). Together, these data suggest that during vasculogenesis, RhoA-ROCK signaling does not regulate apical junction clearance or lumen formation, but instead stimulates EC contractility to restrain EC spreading and therefore vessel dilation.

Arhgap29 and Rasip1 cooperate to suppress RhoA-mediated EC contractility

Given that an important role ascribed to Rasip1 is suppression of RhoA via Arhgap29, we investigated the role of Arhgap29 during lumenogenesis. Rasip1 and Arhgap29 have both been shown to inhibit RhoA activity in vitro, as knockdown of either protein in cultured ECs causes elevated RhoA activity and failed lumen formation[5, 9, 12]. To determine if Arhgap29, or inhibition of RhoA activity, is necessary for blood vessel tubulogenesis, we generated mice with the fourth and fifth exons of Arhgap29 floxed (KOMP). Arhgap29 floxed mice were crossed to Sox2-Cre, which expresses Cre in all epiblast cells (embryo proper)

(Arhgap29^{Sox2KO}). Following recombination, Arhgap29 protein is truncated and non-functional.

Arhgap29^{Sox2KO} embryos died at midgestation (E9–E10) due to failure of chorioallantoic fusion (Online Figure VII A–B''). In situ hybridization of Arhgap29 showed enrichment in ECs as well as the allantois in wild type embryos (Online Figure VII C–F'). Arhgap29^{Sox2KO} embryos displayed normal vascular tubulogenesis, although lumens became narrower by E8.75-9.0 (Figure 4A–D). Mutant ECs exhibited normal polarity, as assessed by apical PODXL, junctional ZO-1, and basal pPaxillin (Online Figure VII G–H'''). In contrast to RhoA or ROCK depletion in ECs, which displayed increased cell spreading (nuclei farther apart), the average distance between Arhgap29 null EC nuclei was decreased by 47% relative to controls, suggesting increased internal contractility (Figure 4B',C',E). To determine whether Rasip1 similarly regulated EC cell shape and contractility, Rasip1$^{f/f}$;Tie2-Cre ECs were assessed. These mice delete Rasip1 several hours after lumen formation[15]. Similar to Arhgap29 mutant vessels, lumens at E8.75 were significantly narrower (Figure 4F–I). In cross sections, the average distance between nuclei was decreased by 30%, suggesting increased EC contractility (Figure 4G–H',J). Thus, Arhgap29 likely acts as a Rasip1 effector to suppress RhoA-ROCK-NMII contractility, enabling controlled vessel expansion.

To assess whether Rasip1-Arhgap29 signaling primarily functions to suppress RhoA activity in order to decrease actomyosin contractility, Rasip1-RhoA double mutants were generated. Control (WT) and RhoA null embryos (ΔRhoA) displayed open lumens, with RhoA-null lumens being slightly larger at these early stages (Figure 4K–L'). Rasip1 null (ΔRasip1) vascular cords exhibited ectopic apical junctions and discontinuous, interrupted lumens (Figure 4M–M', P). Interestingly, Rasip1-RhoA double mutant (ΔRasip1ΔRhoA) embryos did not rescue adhesion remodeling within vascular cords (Figure 4N–N', P), but did increase lumen area, therefore partially rescuing lumen formation (Figure 4O–O', Q). This finding suggests that downstream of Rasip1, suppression of RhoA-ROCK activity by Arhgap29 is not necessary for lumenogenesis or apical adhesion remodeling. Instead, the RhoA signaling axis contributes to tension control and internal contractility in ECs, thereby regulating EC spreading and ultimate lumen size.

NMII acts downstream of Cdc42-Pak4 to remodel apical adhesions, while serving as a RhoA-ROCK effector to regulate apical membrane tension

Both Cdc42 and RhoA signaling pathways promote NMII activity, yet appear to have opposing influences on lumen formation. We hypothesized that these two pathways are spatiotemporally distinct, governing different steps of lumen opening. Specifically, we speculated that Cdc42 activates NMII at cell-cell adhesion complexes to clear them from cord centers, while RhoA activates NMII at the apical membrane after lumen formation to provide membrane tension.

To parse out the roles of Cdc42, RhoA and NMII downstream of Rasip1, we examined NMII activity (pMLC Ser19) during adhesion remodeling and lumen expansion. We found pMLC reduced at cell-cell adhesions in Rasip1 or Cdc42 mutant cords, as well as cords in Pak4-inhibited WECs (Figure 5A–F'). In line with its later role, a transient pool of active NMII is

observed at the apical membrane (Online Figure VII I–K''). Deletion of RhoA inhibited apical membrane pMLC, subsequent to lumen opening (Figure 5G–H'''). By contrast, deletion of Rasip1 or Arhgap29 led to increased activity of pMLC at the apical membrane (Figure 5I–L''). This suggests that upon Rasip1 loss, activated RhoA induces NMII and thus apical membrane contractility. Consistent with this idea, RhoA-deleted ECs displayed a decrease in cell circularity, indicating decreased EC contractility (Figure 5M), while Rasip1 and Arhgap29 deleted ECs had increased circularity (Figure 5N–O). These data provide evidence that Cdc42-Pak4-dependent NMII activity remodels EC adhesions during lumen opening, whereas RhoA-ROCK-dependent NMII activity promotes apical membrane tension to control lumen diameter.

Cdc42, Pak4 and NMII pathway downstream of Rasip1 supports EC-EC junctions

To carry out spatio-temporal analysis of lumenogenesis, we utilized in vitro systems. To study clearance of adhesions during lumen opening, we modeled adhesion development in vitro. When forming adhesions in vitro, ECs must first find each other, then overlap actin-rich cell processes (also called junctional protrusions[23]) before ultimately establishing mature adhesions. As EC adhesions mature, they become smooth and continuous, and actin filaments remodel from perpendicular to parallel relative to the cell-cell interface. We speculated that the remodeling that takes place in vitro is analogous to adhesion remodeling within vascular cords in vivo. We thus siRNA depleted or inhibited signaling proteins downstream of Rasip1, including Cdc42, Pak4, NMHCIIA, RhoA, or ROCK in MS1 cells, and assessed EC adhesion integrity. Depletion of RhoA or ROCK did not affect the integrity of EC adhesions as assessed by VEcad and F-actin staining (Online Figure VIII A–E). However, depletion or inhibition of Rasip1, Cdc42, Pak4, or NMHCIIA resulted in dramatically disrupted adhesions (Figure 6A–H'', Online Figure VIII E). This phenocopied disruption of junctions observed in vivo[15]. Compared to control adhesions with smooth VEcad and F-actin distribution, depleted cells exhibited discontinuous adhesions. Furthermore, F-actin bundles did not align with the cell-cell interface. Thus, adhesion remodeling in vitro recapitulates the in vivo process, where Rasip1-Cdc42-Pak4-NMII signaling regulates vascular adhesion organization, whereas RhoA-ROCK signaling does not. Additionally, these results suggest that this process is regulated by NMII control of F-actin at EC cell-cell adhesions.

To test whether disruption of adhesions by NMII depletion or inhibition correlates with failed lumen formation in vitro, 3D lumen formation assays were performed in the presence of blebbistatin, or siNMHCIIA, siNMHCIIB, or both. Treatment of HUVEC with 10–20μM blebbistatin or siNMHCIIA blocked lumen formation in 3D collagen matrices (Figure 6I–J). Reduction of NMHCIIA and NMHCIIB together prevented lumen formation more efficiently than NMHCIIA or NMHCIIB reduction alone (Figure 6K). These results show that NMII is vital for EC tubulogenesis. NMII is regulated by several proteins that are directly controlled by Cdc42, Rac1, and RhoA, including Pak2, Pak4, MRCKβ and ROCK[10, 23]. To determine which proteins control NMII-dependent lumen formation, we depleted each protein in HUVEC and performed 3D lumen formation assays. Only reduction of the Cdc42 effectors Pak2, Pak4, or MRCKβ prevented lumen formation (Figure 6L–Q).

Thus, both our in vivo and in vitro data suggest that only the Cdc42-NMII pathway, and not the RhoA-ROCK-NMII pathway, regulates NMII-dependent lumen formation.

NMII temporally stimulates lumen formation, then suppresses cell spreading and lumen expansion via RhoA-ROCK signaling

Because NMII activity was first identified within cord adhesion complexes in a Cdc42-Pak4-dependent manner and later at the apical membrane in a RhoA-ROCK-dependent manner, we hypothesized that Cdc42-Pak4-dependent NMII activity regulates adhesion remodeling prior to lumen opening, whereas RhoA-ROCK-dependent NMII activity regulates subsequent apical membrane constriction. To directly test this timing issue in vitro, we inhibited total NMII activity with blebbistatin or RhoA-dependent NMII activity using the ROCK inhibitor Y-27632, either before (0–72hrs) or after (48–72hrs) lumen formation in a 3D lumen formation assay. We reasoned that early blebbistatin-mediated NMII inhibition would block Cdc42-dependent NMII activity in cords, while later ROCK inhibition would block RhoA-dependent NMII activity after lumen opening. We found that treatment with blebbistatin prevented lumen formation, only when treated at the onset of the assay, but did not affect blood vessel lumen size when treated 48hrs after lumen opening (Figure 7A). By contrast, inhibition of ROCK had no influence on lumen formation, but instead led to larger vessel diameters when treated 48hrs after lumen opening (Figure 7A). These results suggest that NMII temporally and spatially controls different aspects of vasculogenesis, downstream of different GTPases. Activated by Cdc42 and Pak4, NMII controls adhesion organization and lumen formation, while downstream of RhoA, NMII controls EC contractility to prevent vessel overexpansion.

To further test if RhoA, ROCK, or NMII regulate cell shape and spreading in vitro, MS1 cells on Matrigel were treated with siRhoA, siNMHCIIA, or with ROCK or NMII inhibitors. Control MS1 cells formed tight EC aggregates after 24 hours when plated at low confluency. RhoA depletion or ROCK inhibition significantly increased overall cell area (spreading), suggesting that these proteins regulate cell shape through the actomyosin machinery (Figure 7B–C, E–F). By contrast, NMIIA depleted or inhibited cells failed to aggregate (Figure 7D, G). Thus, total NMII (including Cdc42-dependent NMII) is necessary for cell-cell adhesion, while a specific NMII pool regulates cell contractility downstream of RhoA-ROCK signaling.

We next asked whether RhoA-ROCK-NMII signaling stimulates EC contractility after lumen formation. MS1 stress fiber development and cell spreading were measured after depletion of RhoA, ROCK or NMII or constitutively active RhoA(V14) overexpression. Indeed, depletion of RhoA, ROCK or NMII activity prevented stress fiber formation and caused ECs to dramatically increase in cell area (Figure 7H–K). Conversely, overexpression of RhoA(V14) caused ECs to greatly contract and create excess stress fibers (Figure 7L–M’). These results suggest that RhoA-ROCK-NMII signaling stimulates EC contractility during blood vessel development.

Lastly, to further test whether NMII controls actomyosin contractility and membrane tension after lumen formation, WEC of embryos with open lumens (2–3 somite stage) were treated with blebbistatin for 2hrs. Control embryos developed aortae with a normal diameter, while

blebbistatin treated embryos exhibited markedly dilated lumens, resembling ROCK inhibited embryos (Figure 7N–O'). To determine how NMII affects lumen area and EC contractility after lumen formation in real time, live imaging Flk1-eGFP yolk sacs was performed in the presence of blebbistatin or the ROCK inhibitor Y-27632. Control vessels maintained a consistent lumen diameter over the course of 40 minutes (Figure 7P–P1' and Online video IX). Treatment with blebbistatin caused vessels to expand by 42% (Figure 7Q–Q1' and Online video X). Treatment of Y-27632 similarly caused vessels to dilate and the vessel area to increase by 37% (Figure 7R–R1' and Online video XII). Close tracking of adjacent ECs showed significant spreading after drug treatment, increasing the space between ECs by 35% after blebbistatin treatment and by 36% after Y-27632 treatment (Figure 7P1-P1', Q1-Q1', R1-R1'). These results demonstrate that NMII possesses a RhoA-ROCK-dependent role, separable from its Cdc42-dependent role, whereby it stimulates EC contractility to suppress lumen dilation. Overall, our data suggest a novel mechanism whereby Rasip1 suppresses apical NMII activity to allow lumen expansion over the course of embryonic growth.

DISCUSSION

In this study, we dissect how Rho GTPase signaling pathways coordinate to regulate distinct cellular events driving blood vessel lumen formation during vasculogenesis (Figure 8, model). Angioblasts first form cell-cell adhesions as they assemble into cords, and thereby establish apicobasal polarity. As EC tubulogenesis initiates, cell-cell adhesions anchored by actin are cleared from the pre-apical membrane and restricted laterally. The EC pre-apical membrane will remodel over time to become a mature apical surface during the tubulogenic process. Reorganization of adhesions in aortic ECs depends on Rasip1 and Cdc42-Pak4-NMII pathway regulation of actin organization. Shortly thereafter, the heart begins to pump plasma into early vessels, expanding nascent lumens. We show that this expansion is controlled by Rasip1 and by the RhoA-ROCK-NMII pathway. NMII and actin are recruited to the apical membrane, where they restrain membrane expansion and lumen size. However, as vessels must grow, Rasip1 balances membrane tension by inhibition of RhoA via Arhgap29. These mechanisms regulate specific cellular events that drive blood vessel formation and expansion in a tightly regulated manner.

Regulation of adhesion organization via Rasip1 and Cdc42-Pak4-NMII

We previously demonstrated that Rasip1 is an essential factor for vascular tubulogenesis. Specifically, we showed that Rasip1 is required for β1- and β3-integrin dependent EC-ECM adhesion, as well as remodeling adhesions away from the EC apical membrane within vascular cords. Moreover, we showed that Rasip1 activates Cdc42 and Rac1, which in turn activate the kinase Pak4. Interestingly, Pak4, as well as myosin light chain kinase (MLCK), is known to control actin contractility by activating NMII, via phosphorylation of pMLC. Previous studies identified roles for Cdc42 and NMII in the building of circumferential actin bundles (CAB) which promote formation of linear and tight AJs[24]. Rasip1 has also been shown to recruit NMIIB to promote endothelial cell-cell adhesion[6]. Reduction of Rasip1 caused EC-EC adhesions to become disrupted, non-linear, and dissociated from actin. These studies suggest that Rasip1-Cdc42-Pak4-NMII signaling promotes adhesion reorganization.

Here, we show that inhibition of Rasip1, Cdc42, Pak4 or NMII suppresses proper adhesion development in vitro. We show that similar mechanisms are at play in vivo, where loss of activity of these components causes failed adhesion redistribution within vascular cords. Whether clearance of junctions in cords (shrinking of junction ribbons) occurs via mechanical 'sliding' along actin tracks to the cord periphery or via actin-based vectorial apical transport of membrane remains unclear. The former is suggested by studies of actomyosin dependent junction remodeling required in numerous morphogenetic processes, such as during *Drosophila* germband extension[25, 26]. Future studies will be necessary to determine whether Rasip1 directly influences adhesions through scaffolding adhesion complexes or actin crosslinking molecules (such as NMII), or whether Rasip1 regulates adhesion integrity solely through signaling and non-scaffolding mechanisms, such as vesicular transport.

Rasip1 and Arhgap29 inhibit RhoA-ROCK-NMII signaling to allow lumen expansion

EC contraction is regulated by actin-myosin contractility, and inhibition of EC contraction leads to cell spreading. The Rap1–Rasip1-Arhgap29 complex has been shown to induce cell spreading by inhibiting RhoA-ROCK-NMII signaling and actin contractility[5, 9, 11, 12]. By suppressing EC contractility, Rasip1 and Arhgap29 may promote cell spreading and allow controlled expansion of vessel lumens, as the embryo grows. Consistent with this idea, deletion of Rasip1 or Arhgap29 after lumen formation causes increased EC contractility and blocks lumen expansion. Conversely, RhoA-ROCK-NMII-dependent actin contractility may normally function to prevent dilation of the lumen by resisting cell spreading. Supporting this, perturbation of RhoA, ROCK, or NMII in vivo after lumen formation leads to dilated vessel lumens. A similar role for the actomyosin contractility machinery in restraint of lumen size has been reported in zebrafish intersomitic vessels, in *Ciona intestinalis* notochord development, and in the developing pancreas[27–29]. In zebrafish, ECs were found to resist plasma membrane deformation (blebbing) via rapid recruitment of myosin and induction of myosin-mediated cortical actin constriction[27]. Thus, we propose that a balance is required, where RhoA-ROCK-NMII signaling stimulates vessel contraction to prevent it from dilating and Rasip1-Arhgap29 suppresses RhoA-ROCK-NMII signaling to allow vessel expansion during growth.

Spatiotemporally distinct roles of NMII through distinct GTPase activities

Our data support the paradigm that Rasip1 controls different pools of GTPases. These, in turn, regulate different pools of NMII to coordinate actomyosin contractility in distinct cellular processes during vessel tubulogenesis. Because both Cdc42 and RhoA signaling pathways promote NMII activity, yet appear to have opposing influences on lumen formation, we sought to clarify the role of these pathways in forming blood vessels. We hypothesized that during EC lumen formation, RhoA controls the activity of an NMII pool at the apical membrane, while Cdc42 controls NMII at cell-cell adhesion complexes. In addition, we predicted that these different functions were likely temporally distinct, given the time course of events during vasculogenesis. This hypothesis finds support in studies which show that the RhoA-ROCK and Cdc42-Pak-MLCK pathways act on distinct pools of NMII[30]. In fibroblasts, MLCK inhibition blocks MLC phosphorylation at the cell periphery, but not the cell center, while ROCK inhibition blocks MLC phosphorylation in the cell

center, but not periphery. Similarly, different GTPases control different subcellular processes: RhoA primarily controls stress fiber development, while Cdc42 controls cell-cell adhesions, membrane ruffling and filopodia[31, 32]. A recent study by Ando et al. showed that RhoA uses NMII to regulate radial stress fiber development into rigid permeable focal adherens junctions, while Cdc42 uses NMII to regulate the development of linear stable adhesions with circumferential bundles of actin[24]. Our findings similarly suggest that different NMII pools come into play at different steps of lumen formation. Temporal inhibition of NMII helped us distinguish its different roles at different time points during vascular lumenogenesis and growth. However, studies on in vivo subcellular distribution of these signaling pathways are still needed and will further our understanding of blood vessel development.

In conclusion, we find that endothelial lumen formation occurs in a step-wise process that is regulated by Rasip1, Rho family GTPases, and NMII. We show here that an essential step in this process is clearance of adhesions from the apical membrane to allow the formation of a single, continuous lumen. We further demonstrate how blood vessel lumen diameter is tightly regulated, to maintain proper lumen size and integrity. Our study uncovers a coordinated action of Rho GTPases governed by Rasip1 to enable proper vasculogenic tubulogenesis.

Supplementary Material

Refer to Web version on PubMed Central for supplementary material.

Acknowledgments

We thank Janet Rossant for Flk1-eGFP, Thomas Carroll for CAG-CreERT2 and Tom Sato for Tie2-Cre mouse lines, and Neal Alto for the Rab5^{CA} construct. We thank Hiromi Yanagisawa for use of cell culture equipment, the TIG group, and the Carroll, Olson, MacDonald, and Cleaver labs for invaluable discussions and assistance. We thank Caitlin Braitsch for critical reading of the manuscript.

SOURCES OF FUNDING

This work was supported by NIH R01HL113498 to DMB, R01HL105606 and R01HL108670 to GED, and CPRIT RP110405 and R01DK079862 to OC.

Nonstandard Abbreviations and Acronyms

AJ	adherens junction
Arghap29	Rho GTPase activating protein 29
β-gal	beta galactosidase
CAG	chicken beta actin promoter/enhancer coupled with cytomegalovirus (CMV) enhancer
Cdc42	cell division control protein 42 homolog
EC	endothelial cell
eGFP	enhanced green fluorescent protein

F-actin	filamentous actin
GTPase	enzyme that hydrolyzes guanosine triphosphate
KOMP	knockout mouse project repository
NMII	Non muscle myosin II (here, NMII-A or NMHCIIA, also myh9; NMII-B, also myh10)
MLCK	myosin light chain kinase
MRCK	myotonic dystrophy kinase related Cdc42-binding kinase
MS1	Mile Sven 1 endothelial line
Pak4	serine/threonine-protein kinase 4
PBS	phosphate buffered saline
PECAM	platelet endothelial cell adhesion molecule 1
PFA	paraformaldehyde
pMLC	phosphorylated myosin light chain
PODXL	podocalyxin
Rab	Ras related protein (here, Rab5; Rab7; Rab11)
Rac1	Ras-related C3 botulinum substrate 1, rho family small GTP binding protein
Rap1	Ras-related protein
Rasip1	Ras interacting protein 1
RhoA	Ras homologue gene family member A
ROCK	Rho-associated protein kinase
siRNA	small interfering RNA
TEM	transmission electron microscopy
Tie2	angiopoietin receptor 2
TJ	tight junction
VE cadherin	vascular endothelial cadherin
WEC	whole embryo culture
ZO-1	zona occludens 1

REFERENCES

1. Iruela-Arispe ML, Davis GE. Cellular and molecular mechanisms of vascular lumen formation. Dev Cell. 2009; 16:222–231. [PubMed: 19217424]
2. Davis GE, Stratman AN, Sacharidou A, Koh W. Molecular basis for endothelial lumen formation and tubulogenesis during vasculogenesis and angiogenic sprouting. Int Rev Cell Mol Biol. 2011; 288:101–165. [PubMed: 21482411]
3. Etienne-Manneville S, Hall A. Rho GTPases in cell biology. Nature. 2002; 420:629–635. [PubMed: 12478284]
4. Bayless KJ, Davis GE. The Cdc42 and Rac1 GTPases are required for capillary lumen formation in three-dimensional extracellular matrices. J Cell Sci. 2002; 115:1123–1136. [PubMed: 11884513]
5. Xu K, Sacharidou A, Fu S, Chong DC, Skaug B, Chen ZF, Davis GE, Cleaver O. Blood vessel tubulogenesis requires Rasip1 regulation of GTPase signaling. Developmental Cell. 2011; 20
6. Wilson CW, Parker LH, Hall CJ, Smyczek T, Mak J, Crow A, Posthuma G, De Maziere A, Sagolla M, Chalouni C, Vitorino P, Roose-Girma M, Warming S, Klumperman J, Crosier PS, Ye W. Rasip1 regulates vertebrate vascular endothelial junction stability through Epac1-Rap1 signaling. Blood. 2013; 122:3678–3690. [PubMed: 23886837]
7. Mitin NY, Ramocki MB, Zullo AJ, Der CJ, Konieczny SF, Taparowsky EJ. Identification and characterization of rain, a novel Ras-interacting protein with a unique subcellular localization. J Biol Chem. 2004; 279:22353–22361. [PubMed: 15031288]
8. Mitin N, Konieczny SF, Taparowsky EJ. RAS and the RAIN/RasIP1 effector. Methods Enzymol. 2006; 407:322–335. [PubMed: 16757335]
9. Post A, Pannekoek WJ, Ponsioen B, Vliem MJ, Bos JL. Rap1 Spatially Controls ArhGAP29 To Inhibit Rho Signaling during Endothelial Barrier Regulation. Mol Cell Biol. 2015; 35:2495–2502. [PubMed: 25963656]
10. Vicente-Manzanares M, Ma X, Adelstein RS, Horwitz AR. Non-muscle myosin II takes centre stage in cell adhesion and migration. Nat Rev Mol Cell Biol. 2009; 10:778–790. [PubMed: 19851336]
11. de Kreuk BJ, Gingras AR, Knight JD, Liu JJ, Gingras AC, Ginsberg MH. Heart of glass anchors Rasip1 at endothelial cell-cell junctions to support vascular integrity. Elife. 2016; 5
12. Post A, Pannekoek WJ, Ross SH, Verlaan I, Brouwer PM, Bos JL. Rasip1 mediates Rap1 regulation of Rho in endothelial barrier function through ArhGAP29. Proc Natl Acad Sci U S A. 2013; 110:11427–11432. [PubMed: 23798437]
13. Strilic B, Kucera T, Eglinger J, Hughes MR, McNagny KM, Tsukita S, Dejana E, Ferrara N, Lammert E. The molecular basis of vascular lumen formation in the developing mouse aorta. Dev Cell. 2009; 17:505–515. [PubMed: 19853564]
14. Strilic B, Eglinger J, Krieg M, Zeeb M, Axnick J, Babal P, Muller DJ, Lammert E. Electrostatic cell-surface repulsion initiates lumen formation in developing blood vessels. Curr Biol. 2010; 20:2003–2009. [PubMed: 20970336]
15. Koo Y, Barry DM, Xu K, Tanigaki K, Davis GE, Mineo C, Cleaver O. Rasip1 is essential to blood vessel stability and angiogenic blood vessel growth. Angiogenesis. 2016
16. Dutta D, Williamson CD, Cole NB, Donaldson JG. Pitstop 2 is a potent inhibitor of clathrin-independent endocytosis. PLoS One. 2012; 7:e45799. [PubMed: 23029248]
17. Willox AK, Sahraoui YM, Royle SJ. Non-specificity of Pitstop 2 in clathrin-mediated endocytosis. Biol Open. 2014; 3:326–331. [PubMed: 24705016]
18. Tapon N, Hall A. Rho, Rac and Cdc42 GTPases regulate the organization of the actin cytoskeleton. Curr Opin Cell Biol. 1997; 9:86–92. [PubMed: 9013670]
19. Zandvakili I, Davis AK, Hu G, Zheng Y. Loss of RhoA Exacerbates, Rather Than Dampens, Oncogenic K-Ras Induced Lung Adenoma Formation in Mice. PLoS One. 2015; 10:e0127923. [PubMed: 26030593]
20. Yang L, Wang L, Zheng Y. Gene targeting of Cdc42 and Cdc42GAP affirms the critical involvement of Cdc42 in filopodia induction, directed migration, and proliferation in primary mouse embryonic fibroblasts. Mol Biol Cell. 2006; 17:4675–4685. [PubMed: 16914516]

21. Zhou X, Florian MC, Arumugam P, Chen X, Cancelas JA, Lang R, Malik P, Geiger H, Zheng Y. RhoA GTPase controls cytokinesis and programmed necrosis of hematopoietic progenitors. J Exp Med. 2013; 210:2371–2385. [PubMed: 24101377]
22. Gu Y, Filippi MD, Cancelas JA, Siefring JE, Williams EP, Jasti AC, Harris CE, Lee AW, Prabhakar R, Atkinson SJ, Kwiatkowski DJ, Williams DA. Hematopoietic cell regulation by Rac1 and Rac2 guanosine triphosphatases. Science. 2003; 302:445–449. [PubMed: 14564009]
23. Barry DM, Xu K, Meadows SM, Zheng Y, Norden PR, Davis GE, Cleaver O. Cdc42 is required for cytoskeletal support of endothelial cell adhesion during blood vessel formation in mice. Development. 2015; 142:3058–3070. [PubMed: 26253403]
24. Ando K, Fukuhara S, Moriya T, Obara Y, Nakahata N, Mochizuki N. Rap1 potentiates endothelial cell junctions by spatially controlling myosin II activity and actin organization. J Cell Biol. 2013; 202:901–916. [PubMed: 24019534]
25. Lecuit T, Yap AS. E-cadherin junctions as active mechanical integrators in tissue dynamics. Nat Cell Biol. 2015; 17:533–539. [PubMed: 25925582]
26. Bertet C, Sulak L, Lecuit T. Myosin-dependent junction remodelling controls planar cell intercalation and axis elongation. Nature. 2004; 429:667–671. [PubMed: 15190355]
27. Gebala V, Collins R, Geudens I, Phng LK, Gerhardt H. Blood flow drives lumen formation by inverse membrane blebbing during angiogenesis in vivo. Nat Cell Biol. 2016
28. Denker E, Sehring IM, Dong B, Audisso J, Mathiesen B, Jiang D. Regulation by a TGFbeta-ROCK-actomyosin axis secures a non-linear lumen expansion that is essential for tubulogenesis. Development. 2015; 142:1639–1650. [PubMed: 25834020]
29. Marty-Santos L, Cleaver O. Pdx1 regulates pancreas tubulogenesis and E-cadherin expression. Development. 2015
30. Totsukawa G, Wu Y, Sasaki Y, Hartshorne DJ, Yamakita Y, Yamashiro S, Matsumura F. Distinct roles of MLCK and ROCK in the regulation of membrane protrusions and focal adhesion dynamics during cell migration of fibroblasts. J Cell Biol. 2004; 164:427–439. [PubMed: 14757754]
31. Nobes CD, Hall A. Rho, rac, and cdc42 GTPases regulate the assembly of multimolecular focal complexes associated with actin stress fibers, lamellipodia, and filopodia. Cell. 1995; 81:53–62. [PubMed: 7536630]
32. Wojciak-Stothard B, Entwistle A, Garg R, Ridley AJ. Regulation of TNF-alpha-induced reorganization of the actin cytoskeleton and cell-cell junctions by Rho, Rac, and Cdc42 in human endothelial cells. Journal of cellular physiology. 1998; 176:150–165. [PubMed: 9618155]
33. Meadows SM, Ratliff LA, Singh MK, Epstein JA, Cleaver O. Resolution of defective dorsal aortae patterning in Sema3E-deficient mice occurs via angiogenic remodeling. Dev Dyn. 2013; 242:580–590. [PubMed: 23444297]
34. Norden PR, Kim DJ, Barry DM, Cleaver OB, Davis GE. Cdc42 and k-Ras Control Endothelial Tubulogenesis through Apical Membrane and Cytoskeletal Polarization: Novel Stimulatory Roles for GTPase Effectors, the Small GTPases, Rac2 and Rap1b, and Inhibitory Influence of Arhgap31 and Rasa1. PLoS One. 2016; 11:e0147758. [PubMed: 26812085]
35. Villasenor A, Chong DC, Cleaver O. Biphasic Ngn3 expression in the developing pancreas. Dev Dyn. 2008; 237:3270–3279. [PubMed: 18924236]
36. Xu K, Chong DC, Rankin SA, Zorn AM, Cleaver O. Rasip1 is required for endothelial cell motility, angiogenesis and vessel formation. Dev Biol. 2009; 329:269–279. [PubMed: 19272373]
37. Koh W, Mahan RD, Davis GE. Cdc42- and Rac1-mediated endothelial lumen formation requires Pak2, Pak4 and Par3, and PKC-dependent signaling. J Cell Sci. 2008; 121:989–1001. [PubMed: 18319301]

Highlights

- Early loss of Rasip1 blocks EC tubulogenesis; later loss of Rasip1 blocks vessel lumen expansion.
- Rasip1/Cdc42/Pak4 activity is required for clearance of apical membrane junctions during tubulogenesis.
- Loss of RhoA or ROCK activity results in vascular lumen overexpansion.
- NMII activity is required early for apical membrane junction clearance (remodeling) and later for restraint of vessel diameter.

Novelty and Significance

What Is Known?

- Murine RASIP1 is necessary in endothelial cells for cell adhesion and the formation of continuous vascular lumens.
- RASIP1 is required for the activity of several GTPase-dependent signaling pathways, including Cdc42, Rac1, RhoA and Rap1.

What New Information Does This Article Contribute?

- Downstream of Rasip1, both Cdc42-Pak and RhoA-ROCK signaling pathways converge on different subcellular pools of non-muscle myosin II (NMII) to drive lumen formation and regulate vessel diameter, respectively.
- Cdc42-Pak4 signaling mediates actomyosin contractility to remodel endothelial cell adhesions at the pre-apical membrane between contacting endothelial cells. This allows the formation of a lumen in blood vessels during vasculogenesis.
- Rasip1 suppression of RhoA-ROCK signaling via Arhgap29 acts later to counter myosin-dependent apical membrane contractility/tension, to allow expansion of lumen diameters.

Understanding the mechanisms of blood vessel lumen formation may further anti-angiogenic approaches that aim to block deleterious vascular growth in diseases such as cancer and diabetic retinopathy. Here, we identify Rasip1 as a promising anti-angiogenesis candidate, which is required for the formation of continuous vascular lumens in growing vessels. Further, we elucidate molecular bottlenecks during vessel formation by dissecting the cellular events that require Rasip1. We show that Rasip1 controls different GTPase signaling pathways that converge upon the actomyosin contractility machinery. We find that different pools of NMII, downstream of Rasip1, control two different processes in endothelial cells: 1. NMII mediates the removal of pre-apical membrane adhesions to form a lumen. 2. NMII then restrains apical membrane expansion, thereby limiting lumen diameter during vessel growth. In the first process, Rasip1 promotes actin contractility via Cdc42 and Pak4 along ribbons of adhesions at the center of EC cords, causing adhesions to clear from the pre-apical membrane. This allows opening of lumens. Subsequently, Rasip1 inhibits NMII and membrane contractility via RhoA suppression to allow regulated lumen expansion. These novel and distinct spatiotemporal molecular and cellular events define the step-wise process of blood vessel morphogenesis and differentiation.

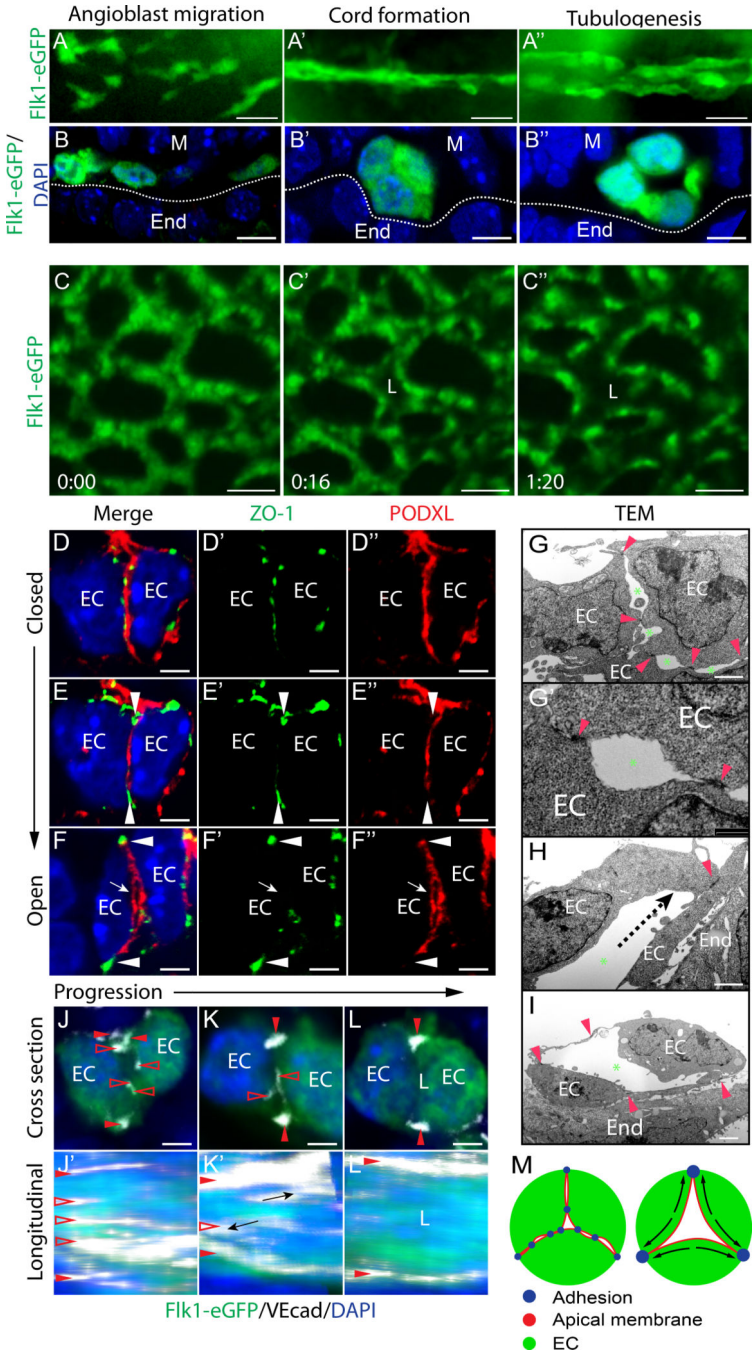

Figure 1. Blood vessel lumens arise between ECs following clearance of pre-apical adhesions

(**A–A’’**) Flk1-eGFP embryos, whole-mount GFP stain (n=3). (**B–B’’**) Cross sections show progression of dorsal aorta cord and lumen formation. (**C–C’’**) Live imaging of Flk1-eGFP yolk sac vasculature. Time in hr:min. (**D–F’’**) Progression of TJs remodeling away from the apical membrane during lumen formation. Tight junctions, ZO-1; apical membrane, PODXL (n>10). EC, endothelial cell; arrowhead, adhesions at periphery; arrow, opening lumen. (**G–I**) TEM of aorta cord and opening lumen. Red arrowheads, EC-EC adhesion complex; green asterisk, luminal spaces between adhesions; dotted line, direction of adhesion movement.

EC, endothelial cell; End, endoderm. (**J–L**) Cross sections of EC cords show adhesion remodeling (clearance from pre-apical membrane). VEcad, white; Flk1-eGFP, green; open arrowheads, clearing junctions at pre-apical membrane; closed arrowheads, sustained peripheral junctions. (**J'–L'**) En face Z-stack confocal image showing apical membrane surface junction ribbons, which are cleared as lumen opens. (**M**) Schematic model of lumen formation: adhesions are rearranged to the cord periphery to form a central lumen. Scale bars: A–A'' 20μm, B–B'' 7μm, C–C'' 25μm, D–F'' 3.5μm, G–I 2μm, J–L 3.5μm.

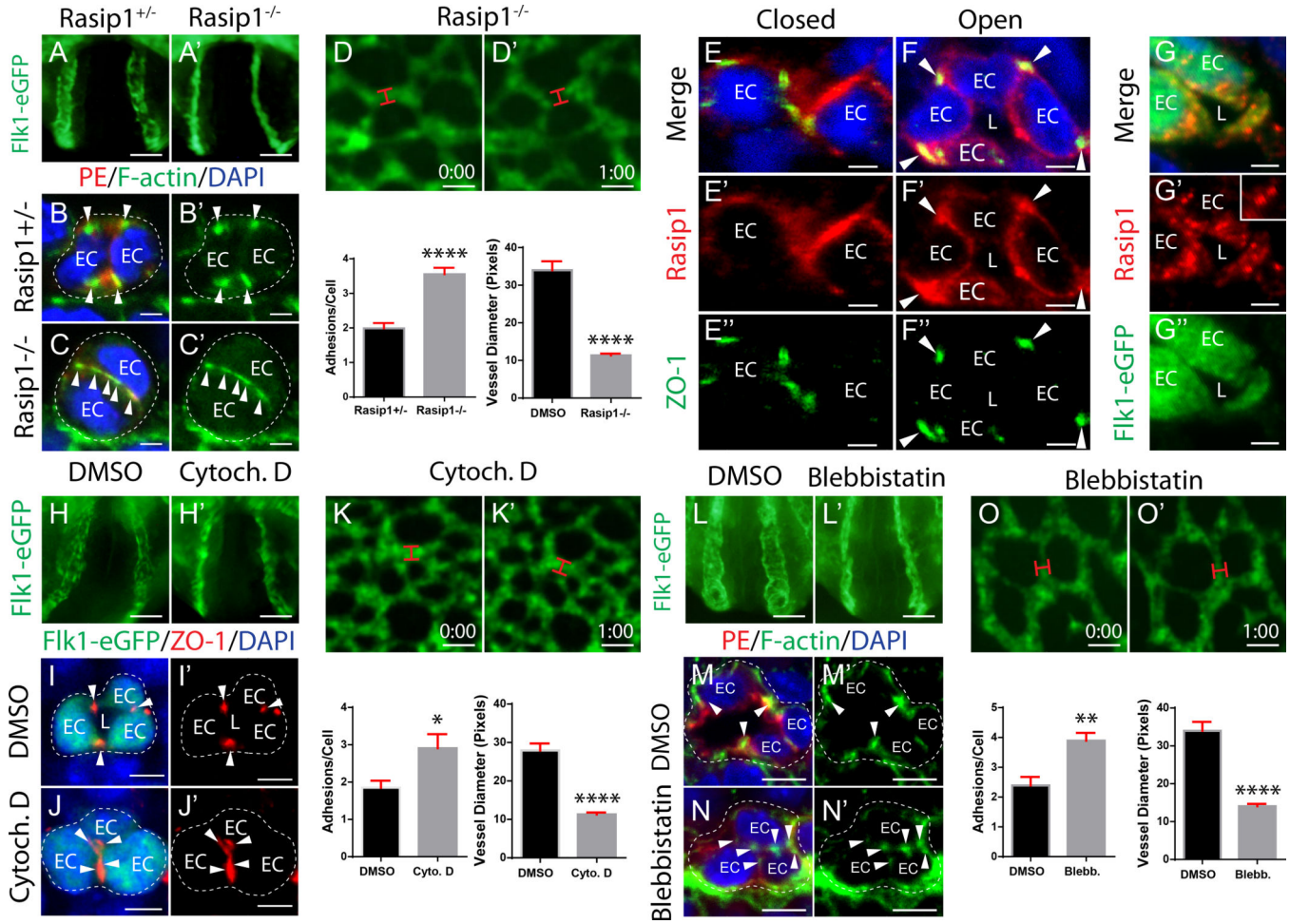

Figure 2. Clearance of EC pre-apical junctions requires Rasip1 and actomyosin contractility

(**A–A'**) Rasip1 null embryos expressing Flk1-eGFP fail to open lumens in the dorsal aorta (n=3 controls, n=3 mutants). (**B–C'**) Cross sections stained with PECAM and Endomucin costain (PE) and F-actin show that Rasip1 mutants fail to remodel adhesions to the periphery of the vascular cord (quantified in graph, n=3 controls, n=3 mutants; 15 Fields of view (FOV)). ****P<0.0001. EC, endothelial cell; arrowhead, adhesion. (**D–D'**) Live imaging of Rasip1−/−;Flk1-eGFP embryo yolk sacs (lumen diameter quantified in graph, n=41 control and n=39 mutant). ****P<0.0001. Red bracket, vessel diameter. Time in hr:min. (**E–F''**) Staining of Rasip1 and TJ marker ZO-1 shows that Rasip1 enriches to adhesions during cord and lumen formation. Arrowheads, adhesions; EC, endothelial cell; L, lumen. (**G–G''**) Staining of Rasip1 localizes at apical membrane after lumen formation. Inset shows endosomal structures. (**H–H'**) WECs treated with Cytochalasin D (10μM) fail to open aortic lumens (n=3 controls, n=3 treated). (**I–J'**) Cross sections stained for GFP and ZO-1 show that Cytochalasin D-treated embryos fail to remodel adhesions to cord periphery (quantified in graph, n=3 controls, n=3 treated; 15 FOV). *P<0.05. (**K–K'**) Live imaging of Cytochalasin D-treated Flk1-eGFP embryos (lumen diameter quantified in graph, n=45 control and n=66 treated). ****P<0.0001. (**L–L'**) WECs treated with blebbistatin (10μM) fail to open aortic lumens (n=3 controls, n=3 treated). (**M–N'**) Cross sections stained with

PE and F-actin show that blebbistatin-treated embryos fail to remodel adhesions to cord periphery (quantified in graph, n=3 controls, n=3 treated; 15 FOV). **P<0.01. (**O–O'**) Live imaging of blebbistatin-treated Flk1-eGFP embryo yolk sacs (lumen diameter quantified in graph, n=41 control and n=20 treated). ****P<0.0001. Scale bars: A–A' 100μm, B–C' 3.5μm, E–E' 25μm, G–G' 3μm, I–I'' 7μm, J–J' 100μm, K–L' 5μm, N–N' 25μm, P–P' 100μm, Q–R' 5μm, T–T' 25μm.

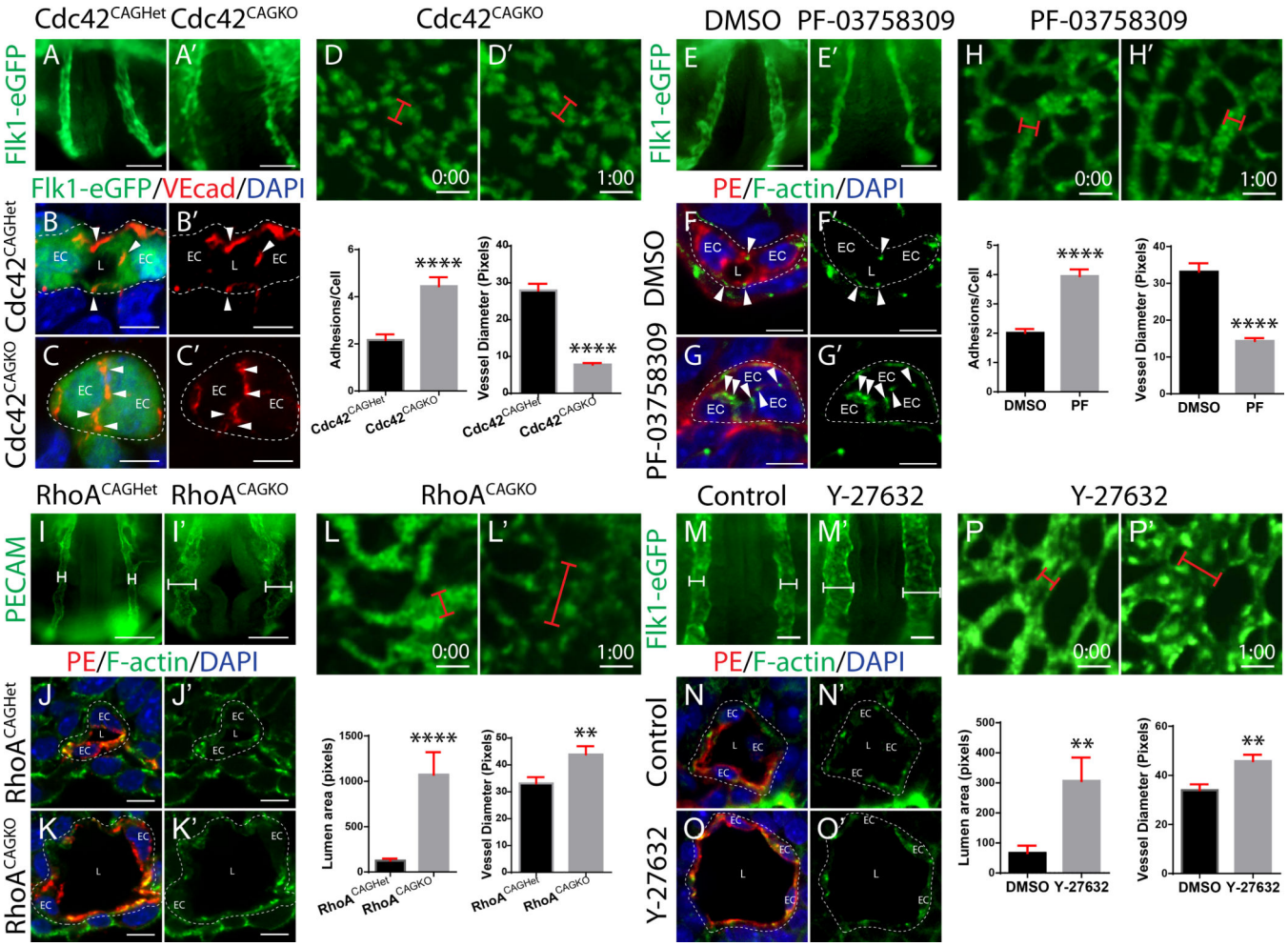

Figure 3. Cdc42, but not RhoA, signaling downstream of Rasip1 is required for lumen formation

(**A–A'**) Cdc42^{CAGKO} embryos expressing Flk1-eGFP fail to open lumens in the dorsal aorta (n>22 controls, n=22 mutants). (**B–C'**) Cross sections stained for GFP and VEcad show that Cdc42^{CAGKO} embryos fail to remodel adhesions to the periphery of the vascular cord (quantified in graph, n=3 control, mutant; 15 FOV). ****P<0.0001. EC, endothelial cell; L, lumen; arrowhead, adhesion. (**D–D'**) Live imaging of Cdc42^{CAGKO} Flk1-eGFP embryo yolk sacs (lumen diameter quantified in graph, n=45 control and n=38 mutants). ****P<0.0001. Red bracket, vessel diameter. (**E–E'**) WECs treated with the Pak4 inhibitor PF-03758309 (10μM) fail to open aortic lumens (n=3 controls, n=3 treated). (**F–G'**) Cross sections stained for PE and F-actin show that Pak4-inhibited embryos fail to remodel adhesions to the cord periphery (quantified in graph, n=3 controls, n=3 treated; 15 FOV). ****P<0.0001. (**H–H'**) Live imaging of Pak4-inhibited Flk1-eGFP embryo yolk sacs (lumen diameter quantified in L, n=40 control and n=33 treated). ****P<0.0001. (**I–I'**) RhoA^{CAGKO} embryos possess expanded dorsal aortae (n=4 controls, n=4 mutants). (**J–K'**) Cross sections stained for PE and F-actin show that RhoA^{CAGKO} embryos fail to maintain proper vessel diameter and possess expanded vessels (quantified in graph, n=8 controls, n=8 mutants, 15 FOV). ****P<0.0001. (**L–L'**) Live imaging of RhoA^{CAGKO} Flk1-eGFP embryo yolk sacs (lumen diameter quantified in graph, n=40 control and n=36 mutant). **P<0.01. (**M–M'**) WECs

treated with Y-27632 (10μM) have expanded vessels (n=3 controls, n=3 treated). (**N–O'**) Cross sections stained for PE and F-actin show that ROCK-inhibited embryos fail to maintain proper vessel diameter and possess expanded vessels (quantified in graph, n=3 controls, n=3 treated, 15 FOV). **P<.01. (**P–P'**) Live imaging of ROCK-inhibited Flk1-eGFP embryo yolk sacs (lumen diameter quantified in graph, n=41 control and n=49 treated). **P<0.01. Scale bars: A–A' 100μm, B–C' 7μm, E–E' 25μm, G–G' 100μm, H–I' 5μm, K–K' 25μm, M–M' 50μm, Q–Q'25μm, S–S' 50μm, T–U' 7μm, W–W' 25μm.

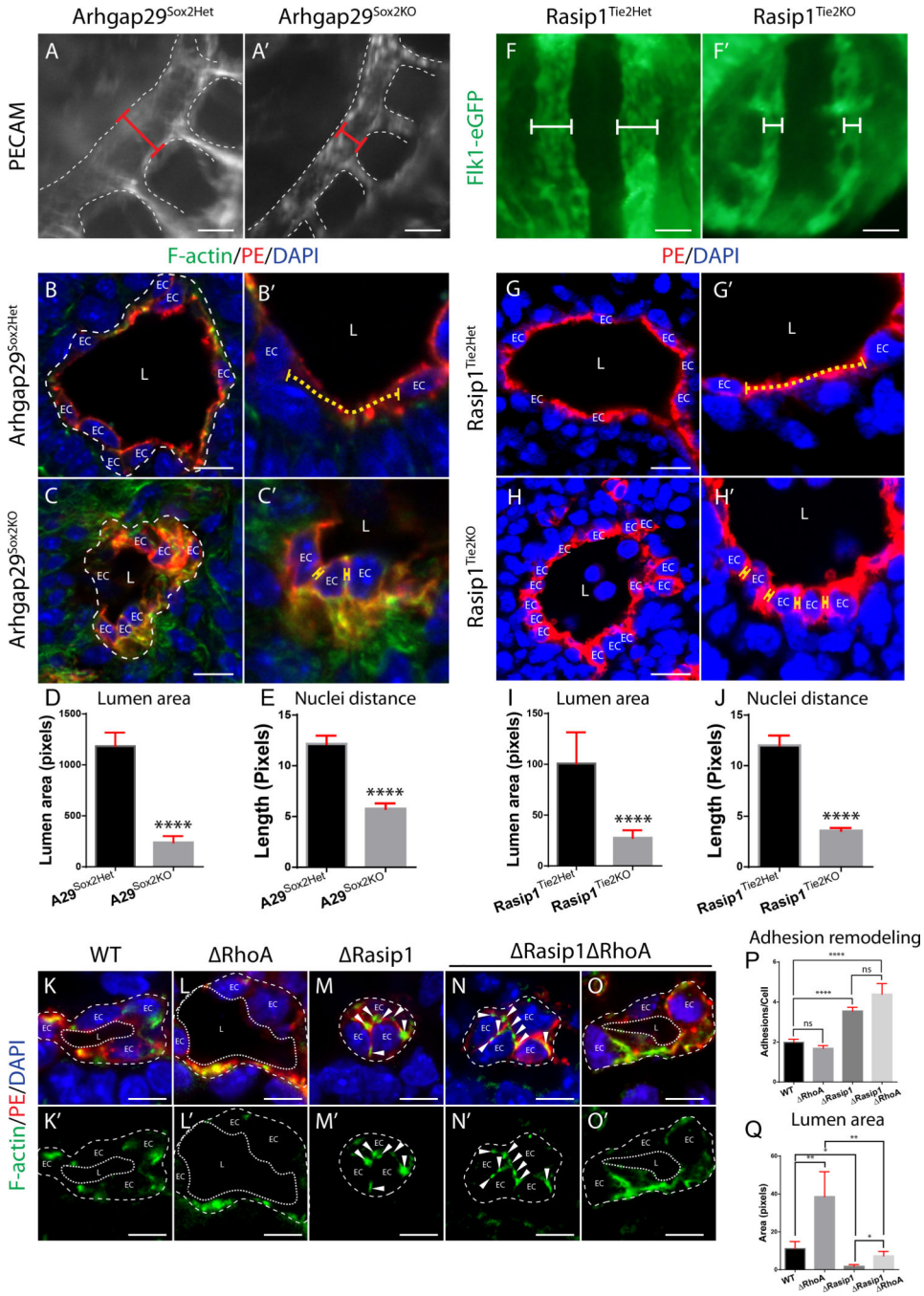

Figure 4. Arhgap29 and Rasip1 cooperate to suppress RhoA-mediated EC contractility and lumen expansion

(**A–A'**) Arhgap29^{Sox2KO} embryos stained with PECAM show constricted dorsal aortae (n=3 control and mutant). Red bracket, diameter of vessel. (**B–C'**) Cross sections of E8.75 Arhgap29^{Sox2het} and Arhgap29^{Sox2KO} embryos shows vessel constriction after Arhgap29 deletion with smaller vessel lumens and closer adjacent EC nuclei (zoomed-in in B' and C', n=3 control and mutant, 15 FOV, quantified in D and E). ****P<0.0001. Yellow dotted line, adjacent nuclei distance; EC, endothelial cell; L, lumen. (**F–F'**) Whole mount images of

Flk1-eGFP;Rasip1^{Tie2Het} and Flk1-eGFP;Rasip1^{Tie2KO} embryos show constricted aortae after Rasip1 deletion. White bracket, diameter of vessel. (**G–H'**) Cross sections of E8.75 Rasip1^{Tie2Het} and Rasip1^{Tie2KO} embryos shows vessel constriction after Rasip1 deletion with smaller vessel lumens and closer adjacent EC nuclei (zoomed-in in G' and H', n= 3 control and mutant, 15 FOV, quantified in I and J). ****P<0.0001. (**K–O'**) Deletion of Rasip1 and RhoA partially rescues lumen expansion but does not rescue adhesion remodeling from the center of vascular cords (n=4 control and mutants, 20 FOV, quantified in P and Q). Arrowheads, adhesion complexes. *P<0.05, **P<0.01, ****P<0.0001, ns =not significant. Scale bars: A–A' 25μm, B–C' 10μm, G–H' 10μm, K–O' 7μm.

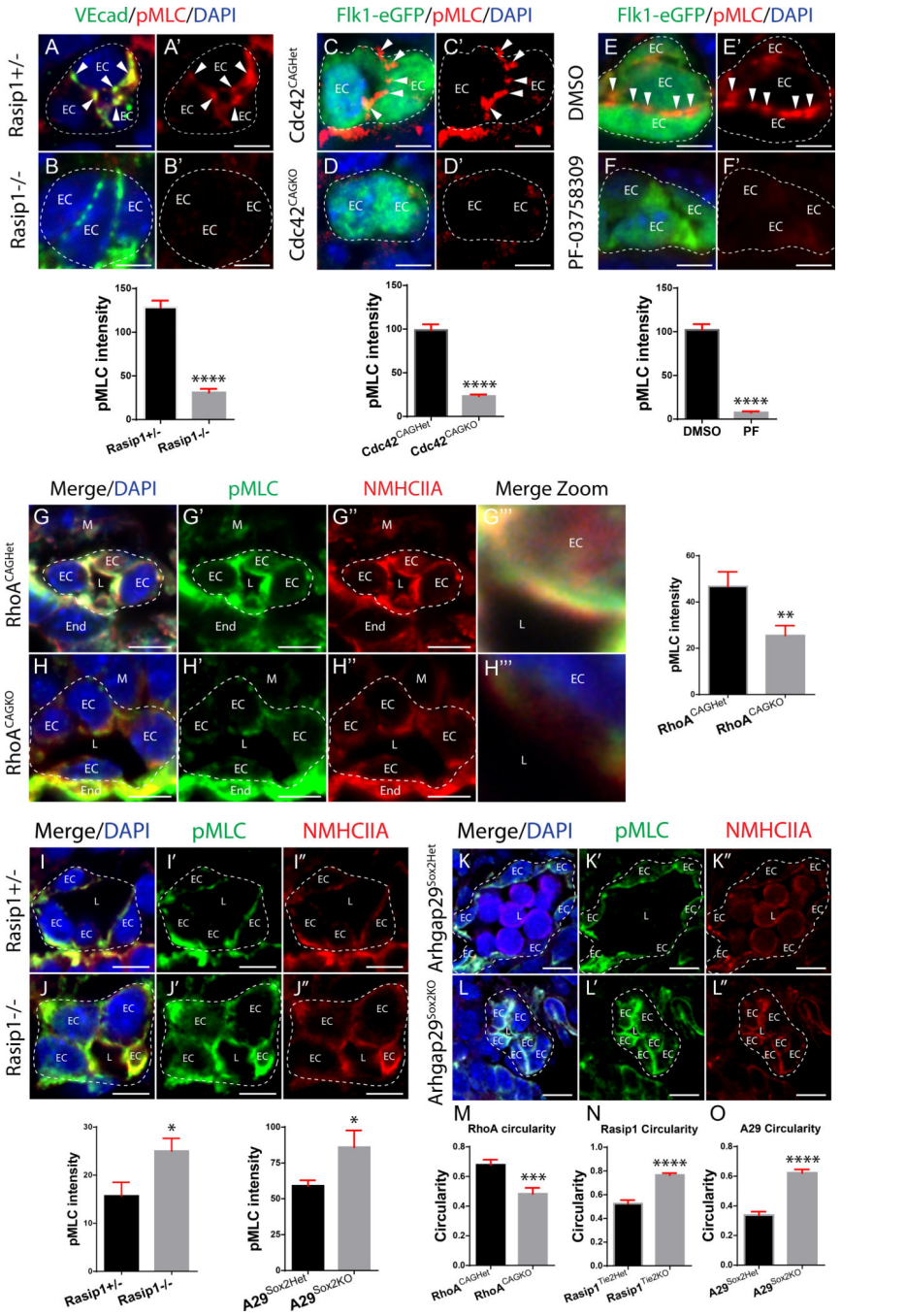

Figure 5. NMII acts downstream of Cdc42-Pak4 to remodel apical adhesions, while serving as a RhoA-ROCK effector to regulate apical membrane tension

(**A–B'**) Staining for VEcad and pMLC on Rasip1+/− and Rasip1−/− embryos shows that Rasip1 is necessary for NMII activity during vascular cord adhesion remodeling (n= 3 control and mutants/WECs, 15 FOV, quantified in graph). ****P<0.0001. Arrowheads, adhesion complex pMLC; EC, endothelial cell. (**C–D'**) Staining of Flk1-eGFP and pMLC on Cdc42^{CAGHet} and Cdc42^{CAGKO} embryos shows that Cdc42 is necessary for NMII activity during cord adhesion remodeling (n= 3 control and mutant, 15 FOV, quantified in

graph). ****P<0.0001. (**E–F'**) Staining of Flk1-eGFP and pMLC on DMSO and PF-03758309-treated WECs shows that Pak4 is necessary for pMLC activity during cord adhesion remodeling (n= 3 control and treated, 15 FOV, quantified in graph). ****P<0.0001. (**G–H'''**) Staining for NMHCIIA and pMLC on $RhoA^{CAGHet}$ and $RhoA^{CAGKO}$ embryos shows that RhoA is necessary for NMII activity at the apical membrane during lumen formation (n= 3 control and mutant, 15 FOV, quantified in graph). **P<0.01. EC, endothelial cell; L, lumen; M, mesoderm; End, endoderm. (**I–J''**) Staining of NMHCIIA and pMLC on Rasip1+/− and Rasip1−/− embryos shows that Rasip1 is necessary to suppress NMII activity at the apical membrane during lumen formation (n= 3 control and mutant, 15 FOV, quantified in graph). *P<0.05. (**K–L''**) Staining of NMHCIIA and pMLC on $Arhgap29^{Sox2Het}$ and $Arhgap29^{Sox2KO}$ embryos shows that Arhgap29 is necessary to suppress NMII activity at the apical membrane during lumen formation (n= 3 control and mutant, 15 FOV, quantified in graph). *P<0.05. (M-O) Quantification of EC circularity after deletion of RhoA, Rasip1, or Arhgap29, respectively (n= 3 control and mutants, 15 FOV). ***P<0.001. ****P<0.0001. Scale bars: A–B' 5μm, D–E' 5μm, G–H' 5μm, J–K'' 7μm, M–N'' 7μm, P–Q'' 10μm.

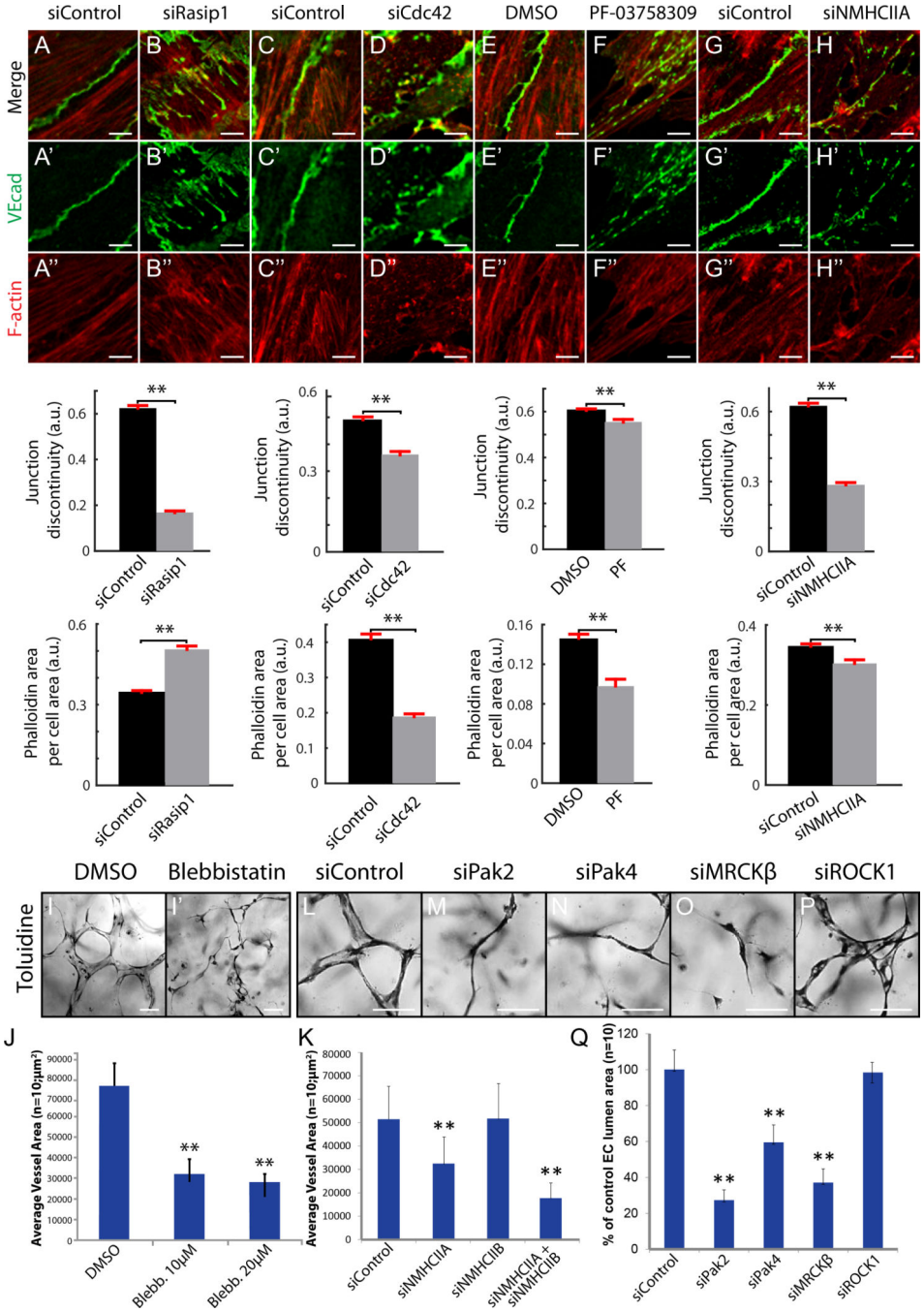

Figure 6. Cdc42, Pak4 and NMII pathway downstream of Rasip1 supports EC-EC junctions and vascular lumenogenesis

(**A–H''**) Staining and quantification of VEcad continuity and F-actin area at MS1 EC cell-cell junctions after siRNA reduction of Rasip1, Cdc42, or NMHCIIA, or pharmacological inhibition of Pak4 (n=3 control and treated, 15 FOV). **P<0.01. (**I–J**) Inhibition of NMII via 10μM or 20μM blebbistatin treatment prevents EC lumen formation in 3D collagen matrices (quantified in J). **P<0.01. (**K**) Graph showing that reduction of NMHCIIA or NMHCIIA and NMHCIIB combined, but not NMHCIIB alone, prevents EC lumen

formation in 3D collagen matrices. **P<0.01. (**L–XQ**) siRNA reduction of Cdc42 effectors Pak2, Pak4, or MRCKβ but not RhoA effector ROCK prevents EC lumen formation in 3D collagen matrices (quantified in Q). **P<0.01. Scale bars: A–N'' 5μm, Q–X 100μm.

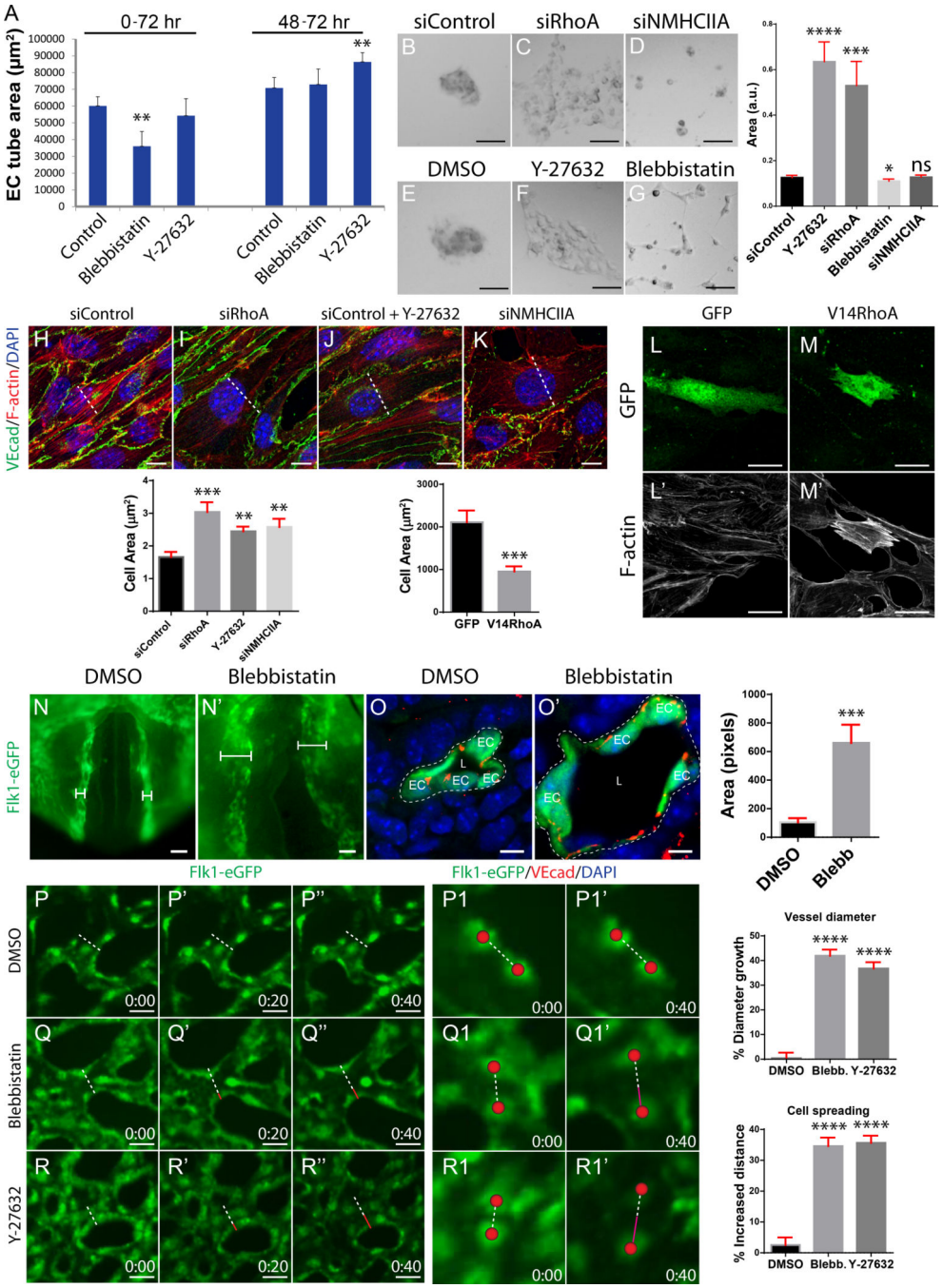

Figure 7. NMII temporally stimulates lumen formation then suppresses cell spreading and lumen expansion via RhoA-ROCK signaling

(**A**) Graph depicting vessel area in a 3D EC lumen formation assay after treatment with blebbistatin or Y-27632 before lumen formation (0–72 hours) or after lumen formation (48–72 hours). **P<0.01. (**B–G**) Matrigel cell aggregation assay after siRNA reduction of RhoA or NMHCIIA or treatment with Y-27632 or blebbistatin (n>50 control and treated, 9 FOV, quantified in graph). *P<0.05, ***P<0.001, ****P<0.0001, ns = not significant. (**H–K**) MS1 cells stained for VEcad and F-actin to assess stress fiber development and cell spreading

after siRNA reduction of RhoA or NMHCIIA or pharmacological inhibition of ROCK (n= 3 control and treated, 15 FOV, cell spreading quantified in graph). **P<0.01, ***P<0.001. Dotted line, lowest central diameter. (**L–M'**) GFP and F-actin staining after adenoviral infection of GFP or V14RhoA + GFP in MS1 cells to assess cell spreading and actin contractility (n>15 control and treated, 15 FOV, cell spreading quantified in graph). (**N–N'**) 2 hour WECs of Flk1-eGFP embryos treated with blebbistatin after initial lumen formation of the dorsal aorta (n=3 control and treated). Brackets, vessel diameter. (**O–O'**) Cross sections show that NMII inhibition after initial lumen formation causes vessels to expand (n=3 control and treated, 15 FOV, quantified in graph). ***P<0.001. EC, endothelial cell; L, lumen. (**P–R''**) Live imaging of Flk1-eGFP yolk sac vessels treated with either blebbistatin or Y-27632 after lumen formation (n= 20 control and treated, change in vessel diameter size quantified in graph). Images are snap shots at 0, 20, and 40 minutes. ****P<0.0001. Dotted line, starting vessel diameter; red line, increased length of vessel diameter. (**P1–R1'**) Tracking of EC spreading after blebbistatin or Y-27632 treatment for 40 minutes (quantified in graph). ****P<0.0001. Red sphere, EC center; dotted line, starting distance between cells; magenta line, increased distance between cells. Scale bars: b–g 50μm, i–l 10μm, n–o' 25μm, q–q' 20μm, R–R' 5μm, T–V'' 25μm.

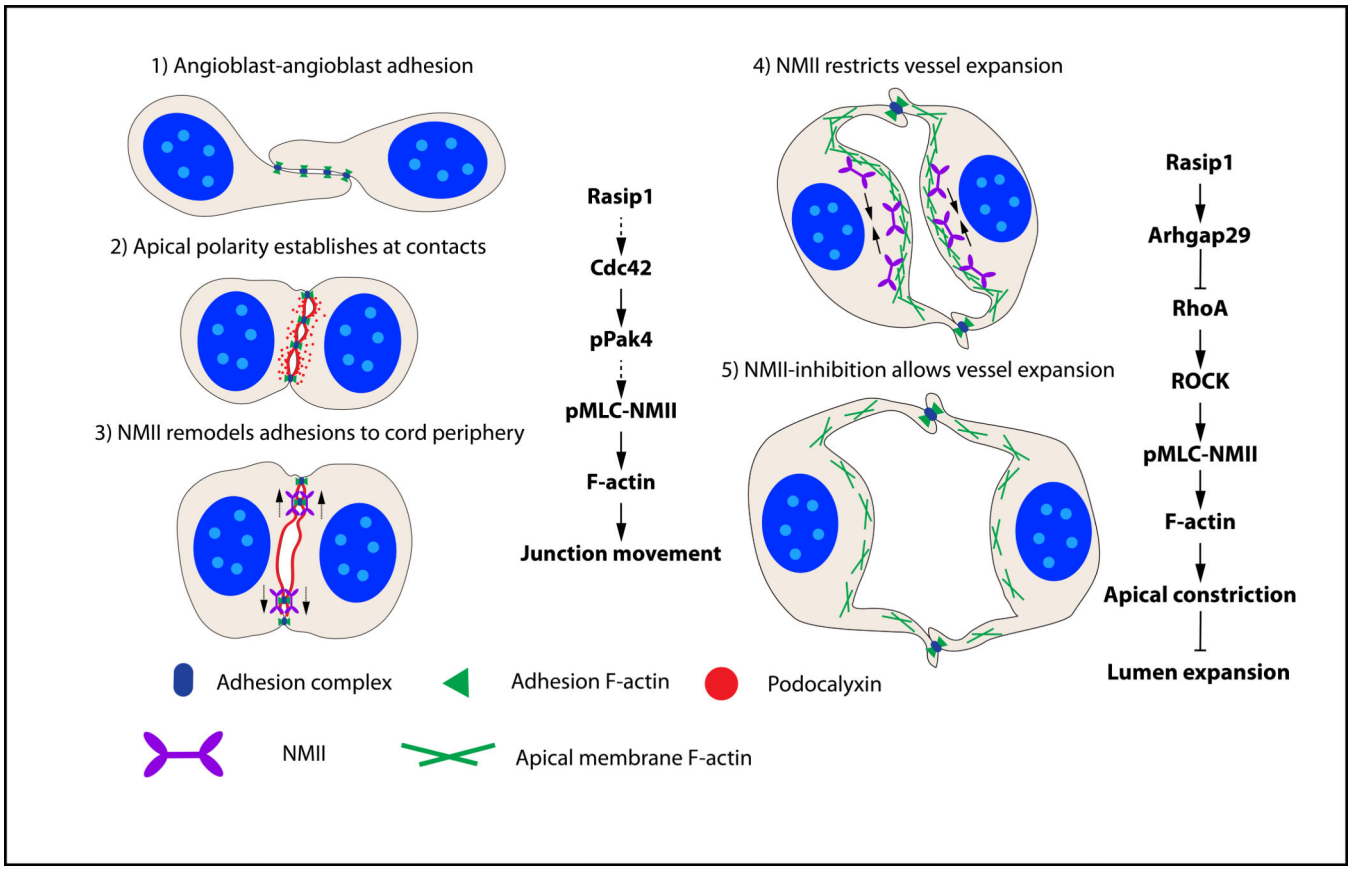

Figure 8. Model of tubulogenesis and vessel expansion during vasculogenesis

1) Angioblasts develop from mesodermal tissue and form punctae of adhesions with adjacent angioblasts. 2) At the angioblast cell-cell contact, PODXL is polarized between the cells, overlapping with the cell adhesion complexes. 3) After activation by Rasip1 and Cdc42-Pak4 signaling, NMII uses its contractile abilities on F-actin to redistribute adhesion complexes away from the pre-apical membrane to the cord periphery, exposing a single luminal space. 4) After lumen formation is complete, the lumen opens in a controlled manner. RhoA-ROCK-activated NMII suppresses excessive expansion of the lumen by constricting F-actin within ECs and at the apical membrane. 5) As the lumen expands, NMII activity is relaxed by inhibiting RhoA-ROCK-NMII signaling through Rasip1 and Arhgap29.